British Journal of Pharmacology (2005) 144, 660–668
www.nature.com/bjp

Responses of the sustained inward current to autonomic agonists in guinea-pig sino-atrial node pacemaker cells

*,[1]Futoshi Toyoda, [1]Wei-Guang Ding & [1]Hiroshi Matsuura

[1]Department of Physiology, Shiga University of Medical Science, Seta-tsukinowacho, Otsu, Shiga 520-2192, Japan

1 The present study was undertaken to examine the responses of the sustained inward current (I_{st}) to β-adrenergic and muscarinic agonists in guinea-pig sino-atrial (SA) node cells using the whole-cell patch-clamp technique. I_{st} was detected as the nicardipine (1 μM)-sensitive inward current at potentials between ~ -80 and $+20$ mV in the presence of low concentration (0.1 mM) of extracellular Ca^{2+}, where the L-type Ca^{2+} current ($I_{Ca,L}$) was practically abolished.

2 β-adrenergic agonist isoprenaline (ISO) in nanomolar concentrations not only increased the amplitude of I_{st} but also shifted the membrane potential producing the peak amplitude (V_{peak}) to a negative direction by $\sim$15 mV without appreciably affecting potential range for the current activation. The stimulatory effect of ISO was concentration-dependent with an EC_{50} of 2.26 nM and the maximal effect (96.4$\pm$22.9% increase, $n=6$) was obtained at 100 nM ISO, when evaluated by the responses at -50 mV.

3 Bath application of acetylcholine (ACh) significantly inhibited I_{st}, which had been maximally augmented by 100 nM ISO; this inhibitory effect of ACh was concentration-dependent with an IC_{50} of 133.9 nM. High concentration (1000 nM) of ACh depressed basal I_{st} by 10.5$\pm$2.0% ($n=3$).

4 In action potential clamp experiments, I_{st} was also detected under control conditions and was markedly potentiated by exposure to ISO.

5 These results strongly suggest that I_{st} not only contributes to the spontaneous action potentials of mammalian SA node cells but also plays a substantial role in mediating autonomic regulation of SA node pacemaker activity.
British Journal of Pharmacology (2005) **144,** 660–668. doi:10.1038/sj.bjp.0706101
Published online 24 January 2005

Keywords: Sustained inward current; sino-atrial node; pacemaker cells; slow diastolic depolarization; isoprenaline; acetylcholine; autonomic regulation; action potential clamp

Abbreviations: ACh, acetylcholine; AV node, atrio-ventricular node; ISO, isoprenaline; I_{st}, sustained inward current; SA node, sino-atrial node

Introduction

The slow diastolic depolarization (pacemaker potential) underlies the spontaneous electrical activity of the pacemaker cells in sino-atrial (SA) node and arises from a complex interaction of multiple ion channels producing either inward or outward current (for a review, see DiFrancesco, 1993; Irisawa *et al*., 1993). It seems most likely that the activation of at least one inward current system together with the decay of the outward K^+ current is primarily responsible for the development of the slow diastolic depolarization. The candidates for the inward current include the hyperpolarization-activated cation current (I_f; DiFrancesco *et al*., 1986), the T-type and L-type Ca^{2+} currents ($I_{Ca,T}$ and $I_{Ca,L}$, respectively; Hagiwara *et al*., 1988; Doerr *et al*., 1989; Verheijck *et al*., 1999; Mangoni *et al*., 2003), the sustained inward current (I_{st}; Guo *et al*., 1995) and the inward background current (I_b; Hagiwara *et al*., 1992), while changes in outward K^+ currents are largely due to the deactivation of the delayed rectifier K^+ current (I_K) composed of the rapidly activating I_{Kr} and/or slowly activating I_{Ks} (Ono & Ito, 1995; Verheijck *et al*., 1995; Lei & Brown, 1996; Ono *et al*., 2000; Matsuura *et al*., 2002).

*Author for correspondence; E-mail: toyoda@belle.shiga-med.ac.jp
Published online 24 January 2005

Previous studies have provided evidence indicating that β-adrenergic agonist isoprenaline (ISO) accelerates the rate of slow diastolic depolarization and thereby increases spontaneous frequency of the SA node automaticity, while the inhibitory effect of acetylcholine (ACh) on SA node electrical activity is primarily mediated through its suppression of the slow diastolic depolarization (DiFrancesco, 1993). Thus, the slow diastolic depolarization phase in SA node pacemaker cells not only plays an important role in generating the spontaneous electrical activity but also represents a relevant target for the chronotropic action of autonomic neurotransmitters. The responses of I_f and $I_{Ca,L}$ to β-adrenergic and muscarinic agonists have been quantitatively examined to elucidate the role of these ionic current systems in mediating the autonomic modulation of heart rate (Zaza *et al*., 1996). The potentiation of I_f and $I_{Ca,L}$ by β-adrenergic agonist ISO occurs over a similar concentration range, suggesting that β-adrenergic response of both I_f and $I_{Ca,L}$ contributes to the acceleration of the slow diastolic depolarization and cardiac pacemaker activity, associated with the elevation of sympathetic tone (Zaza *et al*., 1996). On the other hand, it has been demonstrated that the potency of ACh for the inhibition of I_f is greater than that for the inhibition of $I_{Ca,L}$ or for the activation of the muscarinic K^+ current, $I_{K,ACh}$ (DiFrancesco

et al., 1989; Zaza *et al*., 1996), which suggests that cholinergic inhibition of I_f is primarily involved in the vagal inhibition of SA node spontaneous activity.

I_{st} has been detected in spontaneously beating single cells of mammalian SA and atrio-ventricular (AV) node as the nicardipine-sensitive inward Na^+ current that is activated but exhibits if any little inactivation during depolarization to the potential range of the slow diastolic depolarization (Guo *et al*., 1995; 1996; 1997; Guo & Noma, 1997; Shinagawa *et al*., 2000). These properties of I_{st} appear to favor the hypothesis that, in SA and AV node cells I_{st} substantially contributes to the development of the slow diastolic depolarization by providing an inward current at negative membrane potentials (Mitsuiye *et al*., 2000; Zhang *et al*., 2002). Although some evidence has previously been presented showing that I_{st} is increased by β-adrenergic stimulation (Guo *et al*., 1995; 1997), autonomic regulation of I_{st} has yet to be fully characterized. The aim of the studies described here was therefore to characterize I_{st} in guinea-pig SA node cells with special interest directed to quantitative evaluation of the responses to β-adrenergic and muscarinic agonists.

Methods

Isolation of SA node cells

All experiments conformed with *the Guide for the Care and Use of Laboratory Animals* published by the US National Institute of Health (NIH Publication No. 85-23, revised 1996) and were approved by the institution's Animal Care and Use Committee.

Single SA node cells were isolated from guinea-pig hearts using an enzymatic dissociation procedure similar to that described previously (Anumonwo *et al*., 1992; Guo *et al*., 1997; Matsuura *et al*., 2002). Briefly, adult Hartley guinea-pigs (250 to 400 g body weight) were deeply anesthetized with an overdose of sodium pentobarbitone (80 mg kg^{-1}, i.p.) and the chest cavity was then opened under artificial respiration. The ascending aorta was cannulated *in situ* and the heart was then excised and mounted on a Langendorff apparatus. The heart was retrogradely perfused at 37°C, initially for 4 min with normal Tyrode solution and then for 4 min with a nominally Ca^{2+}-free Tyrode solution. This was followed by 8–12 min perfusion with a nominally Ca^{2+}-free Tyrode solution containing 0.4 mg ml^{-1} collagenase (Wako Pure Chemical Industries, Osaka, Japan). Thereafter, the digested heart was removed from a Langendorff apparatus, and the SA node region, bordered by the crista terminalis, the intra-atrial septum and cranial and caudal vena cava, was dissected out and cut perpendicular to the crista terminalis into small strips measuring about 0.5 mm in width. These tissue strips of the SA node were subjected to another 20 min of digestion in nominally Ca^{2+}-free Tyrode solution containing 1.0 mg ml^{-1} collagenase (Wako) and 0.1 mg ml^{-1} elastase (Roche Diagnostics GmbH, Mannheim, Germany) on a shaking water bath at 37°C. Finally, the enzyme-digested SA node strips were transferred to ~10 ml of a high-K^+, low-Cl^- Kraftbrühe (KB) solution (Isenberg & Klöckner, 1982) in a 35-mm culture dish, and single cells were dispersed by mechanically agitating tissue strips with a fire-polished glass pipette for 10–20 min. Cells were stored in this solution at 4°C for experimental use within 8–10 h.

Solutions and drugs

Normal Tyrode solution contained (in mM): 140 NaCl, 5.4 KCl, 1.8 $CaCl_2$, 0.5 $MgCl_2$, 0.33 NaH_2PO_4, 5.5 glucose and 5.0 HEPES (pH adjusted to 7.4 with NaOH). The nominally Ca^{2+}-free Tyrode solution used for the cell isolation procedure was prepared by simply omitting $CaCl_2$ from the normal Tyrode solution. The Cs^+-substituted, K^+-free Tyrode solution contained (in mM): 140 NaCl, 5.4 CsCl, 1.8 $CaCl_2$, 0.5 $MgCl_2$, 0.33 NaH_2PO_4, 5.5 glucose and 5.0 HEPES (pH adjusted to 7.4 with NaOH). The low-Ca^{2+}, Cs^+-substituted, K^+-free Tyrode solution contained (in mM): 140 NaCl, 5.4 CsCl, 0.1 $CaCl_2$, 0.5 $MgCl_2$, 0.33 NaH_2PO_4, 5.5 glucose and 5.0 HEPES (pH adjusted to 7.4 with NaOH). Agents added to the external solutions included nicardipine (Sigma Chemical Co., St Louis, MO, U.S.A.), ISO (Sigma) and ACh (Sigma). Nicardipine was prepared as a 1 mM stock solution in DMSO and then was diluted at a final concentration of 1 μM in the external solution. ISO was prepared as a 1 mM stock solution in distilled water containing the same concentration of ascorbic acid. ACh was dissolved in distilled water as a 10 mM stock solution. The K^+-rich pipette solution contained (in mM): 70 potassium aspartate, 50 KCl, 10 KH_2PO_4, 1 $MgSO_4$, 3 Na_2-ATP (Sigma), 0.1 Li_2-GTP (Roche), 5 EGTA, 2 $CaCl_2$ and 5 HEPES (pH adjusted to 7.2 with KOH). The Cs^+-rich pipette solution contained (in mM): 125 CsOH, 20 tetraethylammonium chloride (TEA-Cl), 1.2 $CaCl_2$, 5 Mg-ATP (Sigma), 0.1 Li_2-GTP (Roche), 5 EGTA and 10 HEPES (pH adjusted to 7.2 with aspartate). The concentrations of free Ca^{2+} in the K^+-rich and Cs^+-rich pipette solutions were calculated to be approximately 10^{-7} M (pCa = 7.0) and 4.8×10^{-8} M (pCa = 7.3), respectively (Fabiato & Fabiato, 1979; Tsien & Rink, 1980). The KB solution for cell preservation contained (in mM): 70 potassium glutamate, 30 KCl, 10 KH_2PO_4, 1 $MgCl_2$, 20 taurine, 0.3 EGTA, 10 glucose and 10 HEPES (pH adjusted to 7.2 with KOH).

Whole-cell patch-clamp technique and data analysis

Isolated SA node cells were either current- or voltage-clamped using the whole-cell configuration of the patch-clamp technique (Hamill *et al*., 1981) with an EPC-8 patch-clamp amplifier (HEKA Elektronik, Lambrecht, Germany). Patch electrodes were fabricated from glass capillaries (1.5 mm outer diameter, 0.9 mm inner diameter; Narishige Scientific Instrument Laboratory, Tokyo, Japan) using a Sutter P-97 microelectrode puller (Novato, CA, U.S.A.), and the tips were then fire-polished using a microforge. Patch electrodes had a resistance of 2.0–3.0 MΩ when filled with either the K^+-rich or Cs^+-rich pipette solution. An aliquot of dissociated cells was allowed to settle onto the glass bottom of a recording chamber (0.5 ml in volume) mounted on the stage of a Nikon TMD-300 inverted microscope. The chamber was then continuously perfused at a constant rate of ~2 ml min^{-1} with normal Tyrode solution.

Whole-cell current was recorded using a square-pulse, voltage ramp or action potential waveform (Doerr *et al*., 1989). The voltage ramp protocols ($dV/dt = 0.5$ V s^{-1}) comprised three phases: an initial 80 mV ascending (depolarizing) phase from −40 mV, a second descending (hyperpolarizing) phase of 160 mV, and then a third phase returning to −40 mV (see inset in Figure 2a). The current–voltage (I–V) relationship was measured during the second descending phase and

averages of three to five consecutive *I–V* relationships are demonstrated in the figures. The action potential waveforms, recorded in separate experiments from guinea-pig SA node cells that were dialyzed with K^+-rich pipette solution, were fed to the command input of the patch-clamp amplifier for use as voltage-clamp signals. Cell membrane capacitance (C_m) was calculated for each cell by fitting the single exponential function to the decay of the capacitive transient resulting from 5 mV hyperpolarizing steps applied from a holding potential of −50 mV (Bénitah *et al*., 1993). The average value for C_m in SA node cells used for the experiments was 44.3 ± 2.2 pF (mean ± s.e.m., $n = 13$). Experiments were carried out at 34–36°C.

Current and voltage signals as well as trigger pulses were stored on digital audiotape using a PCM data recorder (RD-120TE, TEAC, Tokyo, Japan). Current signals obtained by square-pulse, voltage ramp and action potential waveforms were low-pass filtered at 500 Hz, sampled at 1.0 kHz with an A/D board (ADX-98, Canopus, Kobe, Japan) installed in a personal computer (PC98RL, NEC, Tokyo, Japan) and analyzed using in-house programs. In each original current trace obtained from square-pulse and action potential waveforms, the zero current level is indicated by dotted line.

All averaged values presented are the mean ± s.e.m., and *n* indicates the number of cells studied. Statistical comparisons were made using the Student's *t*-test, and the differences were considered significant at $P < 0.05$.

Results

Properties of nicardipine-sensitive inward currents in guinea-pig SA node cells

As has previously been reported (Anumonwo *et al*., 1992; Guo *et al*., 1997; Matsuura *et al*., 2002), only small percentage (~5%) of cells isolated from SA node regions of the guinea-pig heart exhibited spontaneous and regular contractions during exposure to normal Tyrode solution. In the present study, these spontaneously active cells were regarded as representing SA node cells and were selected for whole-cell patch-clamp recordings. We first analyzed the properties of the membrane currents that were sensitive to inhibition by 1 μM nicardipine in guinea-pig SA node cells. In these experiments, the K^+ currents were minimized by dialyzing the cells with a Cs^+-rich pipette solution, and I_f was inhibited by adding Cs^+ in place of K^+ to the bath solution (the Cs^+-substituted, K^+-free Tyrode solution). The cell membrane was held at −80 mV and then depolarized for 1 s to test potentials between −70 and +20 mV in 10 mV increments. Figure 1a demonstrates a representative example of the current traces in response to these command steps before (upper panel) and during exposure to 1 μM nicardipine (middle panel), as well as the nicardipine-sensitive difference currents obtained by digital subtractions of the corresponding current records at each test potential (lower panel). The nicardipine-sensitive inward current can be detected over the entire range of depolarizing test potentials applied from a holding potential of −80 mV (Figure 1a, lower panel). Figure 1b illustrates the *I–V* relationships for the late current levels measured near the end of 1-s depolarizing voltage-clamp steps, before (control) and during exposure to 1 μM nicardipine. As demonstrated in Figure 1c, the late current levels for the nicardipine-sensitive current was inward over the entire voltage range examined.

The nicardipine-sensitive inward current exhibited a rather sustained activation at test potentials ranging between −70 and −50 mV (Figure 1a, lower panel), which appears to primarily represent the activation of I_{st} but not that of $I_{Ca,L}$, since $I_{Ca,L}$ is typically evoked upon depolarization positive to a threshold of ~−50 mV and represents a time-dependent current decay arising from channel inactivation during depolarizations (Hagiwara *et al*., 1988; Petit-Jacques *et al*., 1993; Guo *et al*., 1996; 1997). On the other hand, the nicardipine-sensitive current recorded at potentials of ⩾−40 mV exhibited a time-dependent decay as expected for the inactivation of $I_{Ca,L}$ but still remained substantially inward even near the end of 1-s voltage-clamp steps.

In order to test the possibility that the activation of I_{st} is also involved, to some extent, in the nicardipine-sensitive inward current activated at test potentials of ⩾−40 mV, the nicardipine-sensitive difference currents were compared in the presence of 1.8 and 0.1 mM extracellular Ca^{2+} in the same SA node cell. In the experiment demonstrated in Figure 1d, the cell membrane was initially depolarized from a holding potential of −80 to −40 mV for 100 ms to inactivate I_{Na} and $I_{Ca,T}$ and then to a test potential of −10 mV to maximally activate $I_{Ca,L}$ (data not shown, see Guo *et al*., 1997). The nicardipine-sensitive current recorded in the presence of 0.1 mM extracellular Ca^{2+} was of small amplitude and exhibited a minimal current decay during depolarizing voltage-clamp step to −10 mV, compared with that recorded in the presence of 1.8 mM extracellular Ca^{2+}. It should be noted that the late current level of the nicardipine-sensitive current measured near the end of a 1-s voltage-clamp step to −10 mV was of similar magnitude in the presence of 1.8 and 0.1 mM extracellular Ca^{2+}. Assuming that $I_{Ca,L}$ is largely removed in the presence of 0.1 mM Ca^{2+} (Guo *et al*., 1997), this experimental result should suggest that the nicardipine-sensitive late current during voltage-clamp step to −10 mV in the presence of 1.8 mM extracellular Ca^{2+} was primarily provided by I_{st} and was little if any related to $I_{Ca,L}$.

We also confirmed, using a double voltage-pulse protocol similar to that shown in Figure 1d, that the amplitude of the nicardipine-sensitive late current measured near the end of depolarizing voltage-clamp steps to other test potentials between −30 and +20 mV was not appreciably affected by reducing the concentration of extracellular Ca^{2+} from 1.8 to 0.1 mM (data not shown), which suggests that $I_{Ca,L}$ scarcely contributes to the nicardipine-sensitive late current at these test potentials. These results are also consistent with the previous observation that $I_{Ca,L}$ undergoes a nearly complete, voltage-dependent inactivation within 1 s during depolarizing voltage steps to these test potentials in the same cell types (Guo *et al*., 1997). It therefore appears that, in the presence of 1.8 mM extracellular Ca^{2+}, I_{st} contributes primarily to the nicardipine-sensitive late current activated at the potential range for the activation of $I_{Ca,L}$ (−30 through +20 mV).

Responses of I_{st} to ISO and ACh

We proceeded to examine quantitatively the responses of I_{st} to ISO and ACh in SA node pacemaker cells to elucidate the autonomic modulation of I_{st}. Since I_{st} appears to be

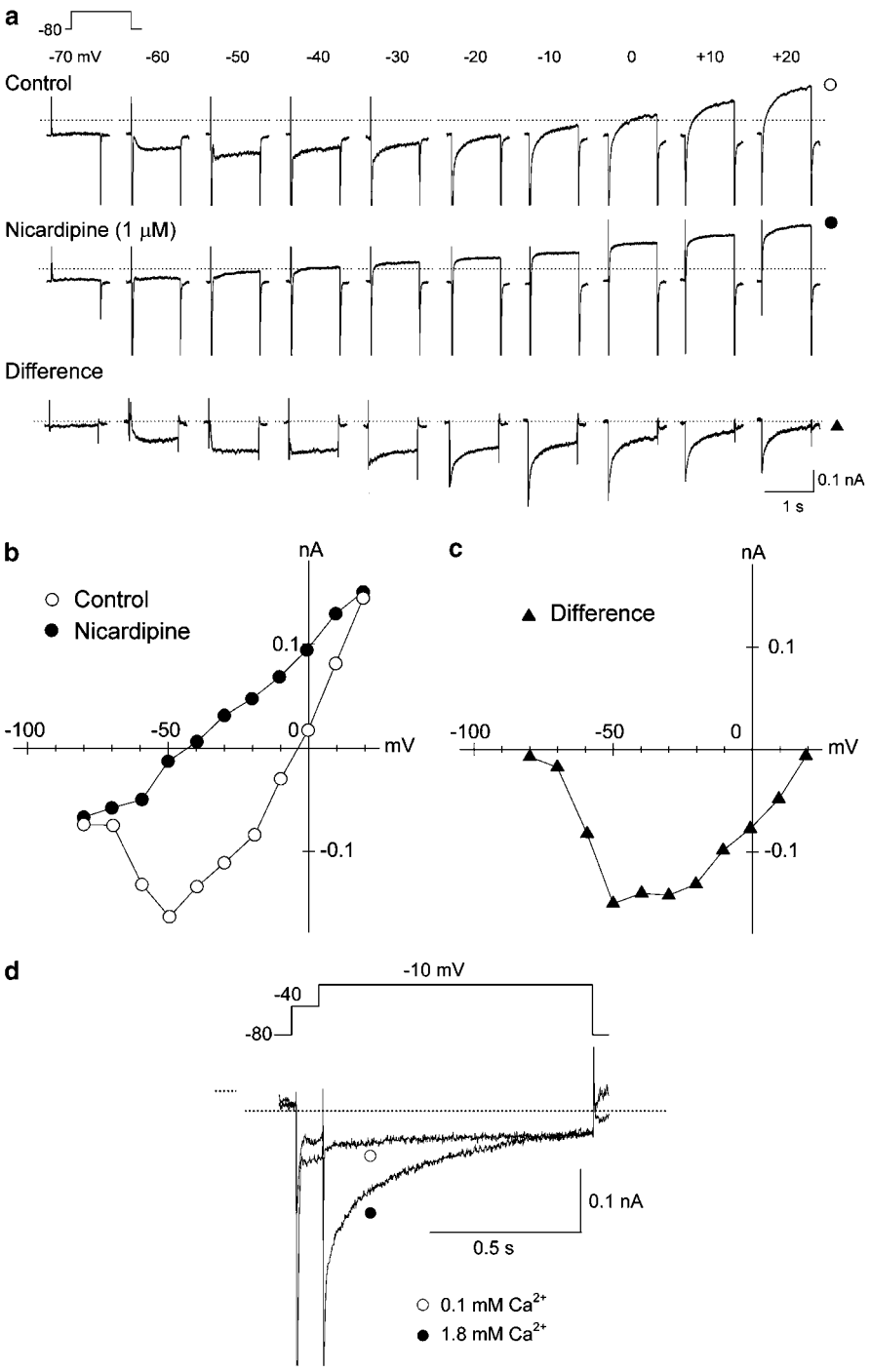

Figure 1 Properties of the nicardipine-sensitive difference currents in spontaneously active SA node cell. (a) Current traces in response to 1 s depolarizing test pulses (up to +20 mV) given from a holding potential of −80 mV under control conditions (upper panel) and during exposure to 1 μM nicardipine (middle panel), and the nicardipine-sensitive difference currents (lower panel) obtained by digital subtraction of the current traces in the presence of nicardipine from those under control conditions. Test potentials are indicated above the control traces. The peaks of I_{Na} were out of scale. (b) *I–V* relationships for the late currents from the records in panel (a), under control conditions and in the presence of nicardipine. Late current levels were measured near the end of each test pulse. (c) *I–V* relationship for the nicardipine-sensitive difference current, measured near the end of the test pulse in records in panel (a). (d) The nicardipine-sensitive difference currents in the presence of 1.8 and 0.1 mM extracellular Ca^{2+}. An SA node cell was initially superfused with the Cs^+-substituted, K^+-free Tyrode solution ($[Ca^{2+}]_o = 1.8$ mM) and then with the low-Ca^{2+}, Cs^+-substituted, K^+-free Tyrode solution ($[Ca^{2+}]_o = 0.1$ mM). The same cell was subsequently superfused with these two solutions but with 1 μM nicardipine. The nicardipine-sensitive currents at 1.8 and 0.1 mM extracellular Ca^{2+} were obtained by digital subtraction of the appropriate current traces in the absence and presence of nicardipine. Voltage-clamp protocol is illustrated above the current traces.

roughly time-independent during square voltage pulses (1 s in duration), I_{st} was measured using the voltage ramp protocol. SA node cells dialyzed with a Cs^+-rich pipette solution were superfused with the low-Ca^{2+}, Cs^+-substituted, K^+-free Tyrode solution, first without and then with ISO at concentrations between 0.1 and 1000 nM. Figure 2a demonstrates a representative example of *I–V* relationships of the membrane currents, recorded in the absence and presence of ISO at 1, 5 and 100 nM, and after addition of 1 μM nicardipine in the presence of 100 nM ISO. In a separate set of experiments, we confirmed that the *I–V* relationship recorded in the presence of 1 μM nicardipine was not appreciably affected by further addition of ISO at any test concentration up to 1000 nM (see Figure 2b). In the experiment of Figure 2a, I_{st} in control conditions was therefore determined as the difference current obtained by subtracting the current trace in the presence of 1 μM nicardipine (plus 100 nM ISO) from that in control, while I_{st} in the presence of ISO at each concentration was obtained by subtracting the current trace in the presence of nicardipine (plus 100 nM ISO) from that in the presence of ISO alone (Figure 2c). ISO at 100 nM markedly increased the amplitude of I_{st} without causing any appreciable change in the

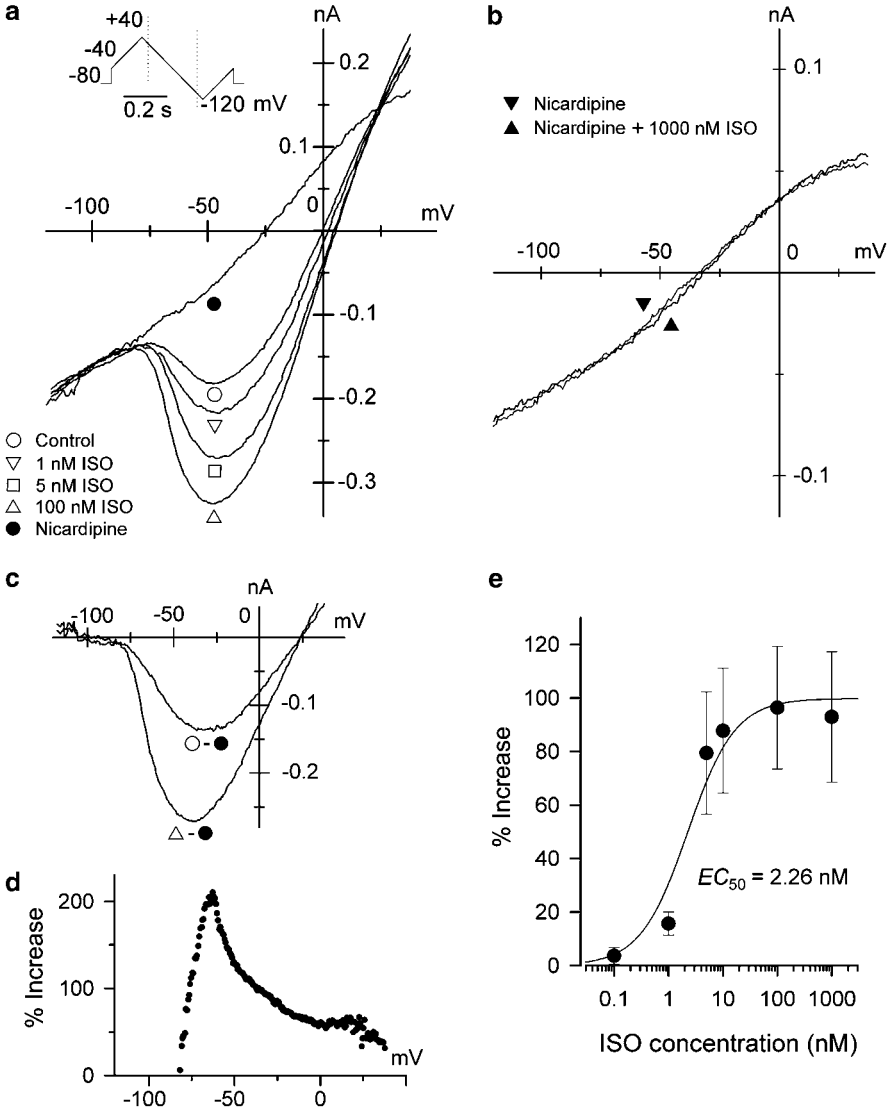

Figure 2 Stimulatory effect of ISO on I_{st}. (a) *I–V* relationships recorded using the voltage ramp protocol from an SA node cell superfused with the low-Ca^{2+}, Cs^+-substituted, K^+-free Tyrode solution, before (control) and during exposure to ISO at concentrations of 1, 5 and 100 nM, and after addition of 1 μM nicardipine in the presence of 100 nM ISO. Inset shows the voltage ramp protocol ($dV/dt = 0.5\,V\,s^{-1}$) used in the experiments and *I–V* relationship was obtained during the ramp from +40 to −120 mV. (b) *I–V* relationships recorded in the presence of nicardipine (1 μM) and nicardipine (1 μM) plus ISO (1000 nM). Panels (a) and (b) were obtained from different cells. (c) *I–V* relationships for I_{st} under control conditions and in the presence of 100 nM ISO, obtained by digital subtraction of the appropriate current records shown in panel (a). (d) Percentage increase in the amplitude of I_{st} by ISO (100 nM) at various potentials, determined as the fractional increase in the amplitude of I_{st} by 100 nM ISO at 1 mV step. (e) Concentration–response relationship for enhancement of I_{st} by ISO at concentrations of 0.1 to 1000 nM. Percentage increase represents the fraction of I_{st} at −50 mV increased by ISO with reference to the control amplitude of I_{st}. Data points are mean ± s.e.m. of six different cells, and the smooth curve represents a least-squares fit of the Hill equation: $R = R_{max}/(1 + (EC_{50}/[ISO]))$, where R_{max} is the fitted maximal response, EC_{50} is a half-maximally effective concentration of ISO (2.26 nM).

potential range for the current activation. However, ISO significantly shifted the membrane potential giving the peak amplitude of I_{st} (V_{peak}) to a negative direction by $\sim$15 mV (control, -27.5 ± 3.2 mV; 100 nM ISO, -42.8 ± 3.1 mV; $n=6$; $P<0.05$). Figure 2d represents the percentage increase in the amplitude of I_{st} evoked by 100 nM ISO at potentials in the range of ~-80 to $+30$ mV, obtained by measuring the fractional increase in the amplitude of I_{st} in the *I–V* curves (Figure 2c) at 1 mV step. The stimulatory effect of ISO on I_{st} was maximal at potentials at around -60 mV. The concentration–response relationship for potentiation of I_{st} by ISO, determined by the responses at -50 mV, was reasonably well described by a Hill equation with an EC_{50} of 2.26 nM (Figure 2e).

We then quantitatively examined whether ACh at concentrations of 1 to 1000 nM produces an inhibitory effect on I_{st} previously stimulated by a maximally effective concentration (100 nM) of ISO in guinea-pig SA node cells. Figure 3a illustrates a representative example of *I–V* relationships obtained using the voltage ramp protocol, before and during exposure to 100 nM ISO and after addition of 100 nM ACh in the presence of 100 nM ISO. In these experiments, SA node cells were finally exposed to 1 μM nicardipine in the presence of ISO and ACh to identify I_{st}. In separate experiments, it was also confirmed that *I–V* relationship recorded in the presence of 1 μM nicardipine was not appreciably affected by the subsequent addition of ACh at any test concentration (up to 1000 nM), together with 100 nM ISO (see Figure 3b). I_{st} in control conditions, in the presence of 100 nM ISO and 100 nM ISO plus 100 nM ACh, was therefore determined by digital current subtraction, using the current trace recorded in the presence of nicardipine (together with 100 nM ISO and 100 nM ACh), and is shown superimposed in Figure 3c. ACh at 100 nM was found to reduce greatly the amplitude of I_{st} prestimulated by 100 nM ISO.

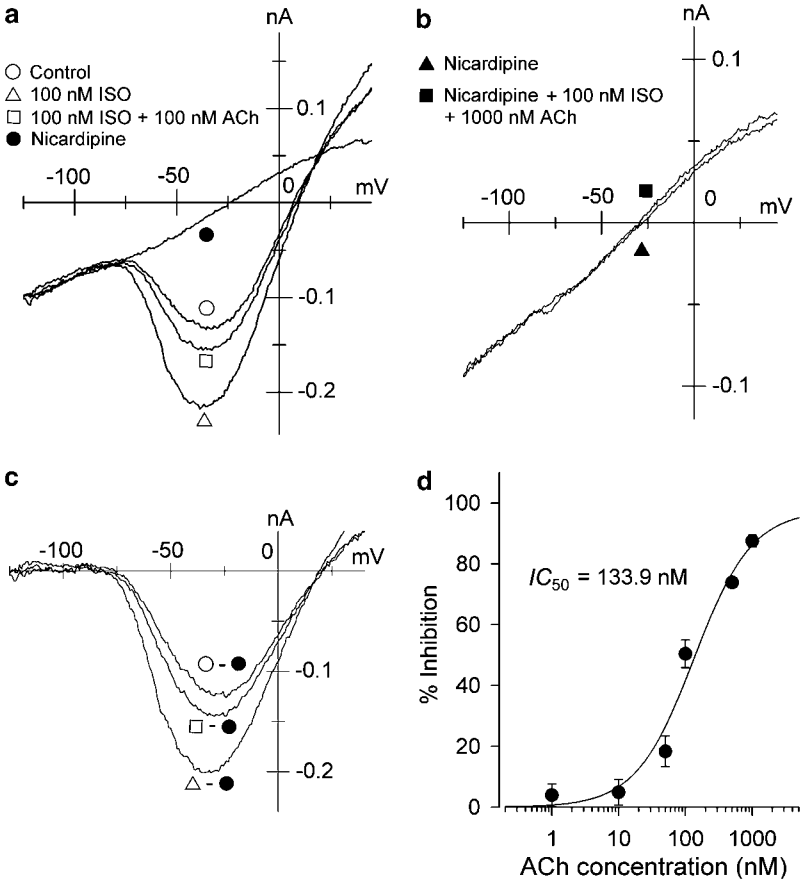

Figure 3 Inhibitory effect of ACh on the ISO-stimulated I_{st}. SA node cells were initially exposed to 100 nM ISO and then to a combination of 100 nM ISO plus ACh at various concentrations ranging from 1 to 1000 nM, and finally to 1 μM nicardipine in the presence of ISO and ACh. (a) *I–V* relationships recorded before (control) and during exposure to 100 nM ISO and 100 nM ISO plus 100 nM ACh, and after addition of 1 μM nicardipine in the presence of ISO and ACh. The voltage ramp protocol was used to record the *I–V* relationships. (b) *I–V* relationships recorded in the presence of 1 μM nicardipine, first without and then with 100 nM ISO plus 1000 nM ACh. Panels (a) and (b) were from different cells. (c) I_{st} under control conditions, in the presence of 100 nM ISO alone and 100 nM ISO plus 100 nM ACh, determined as the nicardipine (1 μM)-sensitive difference current by digital subtraction of the appropriate current records shown in panel (a). (d) Concentration-dependent inhibition of ISO (100 nM)-induced I_{st} by ACh at concentrations of 1 to 1000 nM. Percent inhibition represents the magnitude of I_{st} inhibited by each concentration of ACh, relative to the amplitude of I_{st} evoked by 100 nM ISO. The amplitude of I_{st} was measured as the nicardipine-sensitive difference current at -50 mV in the *I–V* curves shown in panel (c). Data points represent the mean$\pm$s.e.m. of four different cells and were fitted to the Hill equation: $R=R_{max}/(1+(IC_{50}/[ACh]))$, where R_{max} is the fitted maximal response, IC_{50} is a half-maximally inhibitory concentration of ACh (133.9 nM).

To assess quantitatively this inhibitory effect of ACh on the ISO-stimulated I_{st}, the amplitude of I_{st} reduced by various concentrations of ACh was measured at −50 mV and was then normalized with reference to the amplitude of I_{st} potentiated by 100 nM ISO at the same potential (percentage inhibition). In Figure 3d, the percentage inhibition thus obtained was plotted as a function of ACh concentration. ACh reduced the amplitude of the ISO-stimulated I_{st} in a concentration-dependent manner with an IC_{50} of 133.9 nM and the maximal effect (87.4±1.2% inhibition, $n=4$) was obtained with 1000 nM ACh.

Bath application of ACh at concentrations of ⩽100 nM was not effective at inhibiting I_{st} without prestimulation by ISO (100 nM), whereas a higher concentration (1000 nM) of ACh evoked a small but significant inhibitory effect on basal I_{st} by 10.5±2.0% ($n=3$).

Contribution of I_{st} *to pacemaker activity as revealed by action potential clamp*

To assess the contribution of I_{st} to SA node pacemaking activity, membrane currents were measured from guinea-pig SA node cells using the action potential waveform as the command for the voltage-clamp (action potential clamp; Doerr *et al*., 1989). Figure 4a demonstrates a representative example of spontaneous action potentials in guinea-pig SA node cells recorded in the current-clamp mode (upper panel) as well as the first derivative of the membrane potential (dV/dt, lower panel). The firing rate of spontaneous electrical activity averaged 178±8 min^{-1} ($n=12$). A characteristic slow depolarization following the repolarization of the preceding action potential led smoothly into the rapid upstroke of the action potential. It thus seems that membrane current systems involved in this slow diastolic depolarization at potentials between ∼−60 and −45 mV play a crucial role in the SA node automaticity (DiFrancesco, 1993; Irisawa *et al*., 1993). The diastolic depolarization rate (DDR) and maximum upstroke velocity of the action potential, obtained by the dV/dt, averaged 130.6±10.9 mV s^{-1} and 7.0±1.2 V s^{-1} ($n=6$), respectively.

Figure 4b illustrates the membrane currents recorded during action potential waveforms shown in Figure 4a as a voltage-clamp command, under control conditions (upper panel), during exposure to 1000 nM ISO (middle panel), and after addition of 1 μM nicardipine (lower panel). I_{st} in control conditions was estimated by digital subtraction of the current trace in the presence of nicardipine plus ISO (lower panel in Figure 4b) from that in control (upper panel), while I_{st} in the presence of ISO was obtained by digitally subtracting the current traces in the presence of nicardipine plus ISO (lower panel) from that in the presence of ISO alone (middle panel). As demonstrated in Figure 4c, I_{st} was detected in control conditions (thick curve, lower panel) and was markedly potentiated by exposure to 1000 nM ISO (thin curve, lower panel), over the entire voltage range (between ∼−64 and ∼+10 mV) of action potential waveforms of SA node cells. In Figure 4d, I_{st} in control conditions and during exposure to 1000 nM ISO is plotted as a function of membrane potential during action potential clamp protocol. I_{st} in control conditions peaked at potentials ∼−20 mV and decreased at more positive and negative potentials, which is largely similar to the voltage dependence of I_{st} recorded using voltage ramp protocol

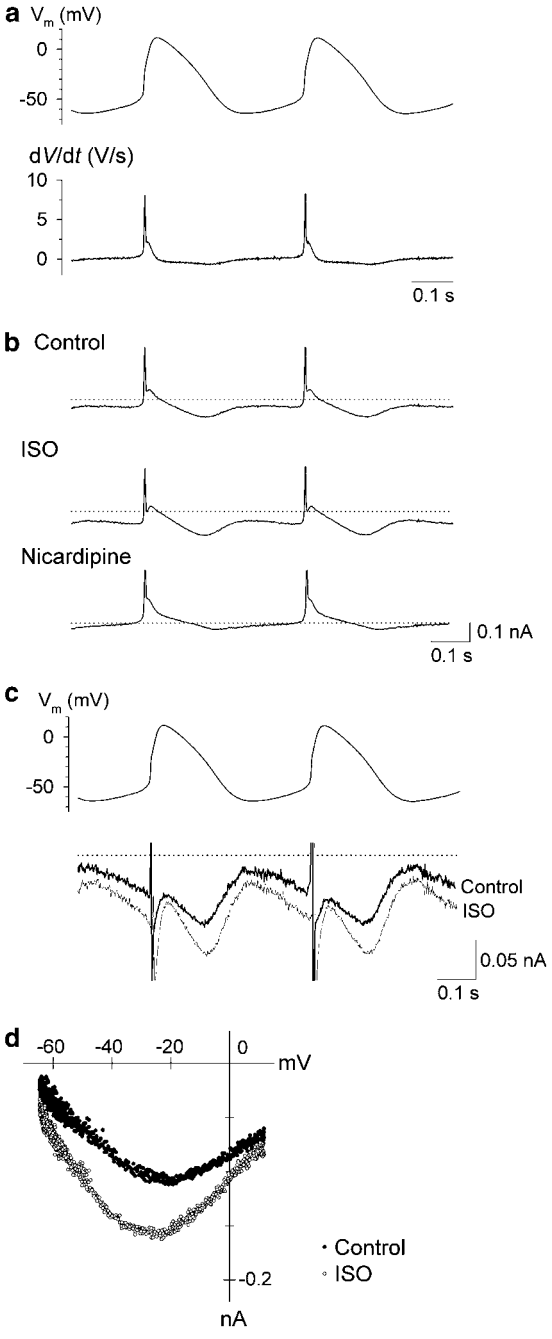

Figure 4 Estimation of the contribution of I_{st} to spontaneous activity of SA node using action potential clamp technique. (a) Spontaneous action potential recorded from a guinea-pig SA node cell superfused with normal Tyrode solution (upper panel) and the dV/dt (lower panel). K^+-rich pipette solution was used. Maximal diastolic potential was −64.3 mV, and the firing rate, 167 min^{-1} in this particular cell. (b) An SA node cell dialyzed with the Cs^+-rich pipette solution was superfused with the low-Ca^{2+}, Cs^+-substituted, K^+-free Tyrode solution. Membrane currents during action potential waveforms shown in panel (a), before (upper panel) and during (middle panel) exposure to 1000 nM ISO, and after addition of 1 μM nicardipine (lower panel). Panels (a) and (b) were obtained from different cells. (c) I_{st}, in the absence (thick curve) and presence of 1000 nM ISO (thin curve), determined as the nicardipine (1 μM)-sensitive difference currents obtained by digital subtraction of appropriate current traces shown in panel (b) (see text). (d) I_{st} in the absence (control) and presence of ISO, plotted as a function of voltage level during action potential waveforms. Data were obtained from the results shown in panel (c).

(Figure 2c). Similarly, ISO potentiated I_{st} at potentials in the range tested and shifted V_{peak} by $\sim$5–10 mV to a negative direction. In a total of three cells, 1000 nM ISO increased the amplitude of I_{st} by 84.7±16.8% when evaluated by the response at −50 mV, which is similar to the value obtained using voltage ramp protocol for 1000 nM ISO (92.9±24.4% increase, $n=4$; Figure 2e).

Discussion

The present study characterizes the nicardipine-sensitive difference currents using depolarizing square voltage steps applied from a holding potential of −80 mV to a wide range of membrane potentials (−70 to +20 mV) in spontaneously beating SA node cells of guinea-pig and provides the evidence to support the view that the nicardipine-sensitive current comprises I_{st} as well as $I_{Ca,L}$ (Figure 1), in agreement with the previous report (Guo *et al*., 1995). The nicardipine-sensitive inward current activated at potentials of −70 to −50 mV is practically time-independent during 1-s depolarizing voltage-clamp steps (Figure 1). Furthermore, the nicardipine-sensitive inward current at these negative potentials has been reported to be dependent upon extracellular Na^+ but not extracellular Ca^{2+} in SA node cells (Guo *et al*., 1996; 1997). Thus, the nicardipine-sensitive inward current at potentials of −70 to −50 mV appears to arise primarily from the activation of the monovalent cation conductance of I_{st} (Mitsuiye *et al*., 2000).

On the other hand, the nicardipine-sensitive inward current at potentials of −40 to +20 mV exhibits a voltage- and time-dependent decay but still remains substantially inward near the end of 1-s voltage-clamp steps. In addition, the amplitude of the late inward current is not appreciably affected (Figure 1) even when the activation of $I_{Ca,L}$ is almost totally abolished by the presence of 0.1 mM extracellular Ca^{2+} (Guo *et al*., 1997), supporting the involvement of I_{st} in the nicardipine-sensitive inward current at these potential levels. It should be noted, however, that I_{st} can be overestimated under the present experimental conditions where the driving force for inward Na^+ conductance through I_{st} is increased by omitting Na^+ from the pipette solution.

Previous studies have examined the role of I_f, $I_{Ca,T}$ or $I_{Ca,L}$ in the slow diastolic depolarization that underlies the spontaneous electrical activity of SA node cells by using the pharmacological tools (Hagiwara *et al*., 1988; van Ginneken & Giles, 1991; Verheijck *et al*., 1999). However, the functional role of I_{st} in SA node automaticity has not been tested experimentally because of the lack of its specific inhibitor (Mitsuiye *et al*., 2000). In the present action potential clamp experiment conducted in the presence of low (0.1 mM) extracellular Ca^{2+} concentration (Figure 4), the nicardipine-sensitive inward current can be detected over the entire voltage range associated with the spontaneous action potentials of SA node cells. Thus, the inward current responsible for the development of the slow diastolic depolarization appears to be contributed, at least to some extent, by the activation of I_{st} in SA node cells. In recent years, mathematical models have also demonstrated that spontaneous frequency of SA node automaticity is increased by 0.6 to 20% when equations for I_{st} are incorporated (Zhang *et al*., 2002). It seems likely that I_{st}, which is expressed in spontaneously active SA node cells of various mammalian species (Guo *et al*., 1995; 1997; Shinagawa *et al*., 2000), is activated and contributes to the SA node automaticity, by providing an inward current over the voltage range corresponding to the slow diastolic depolarization. It is interesting to note that the *I–V* relationship for I_{st} exhibits a negative slope over the potential range for the slow diastolic depolarization (Figures 2c, 3c and 4d), which is expected to constitute a positive feedback loop to depolarize the cell membrane during the diastolic phase in SA node cells.

Bath application of the β-adrenergic agonist ISO in nanomolar concentrations not only increases the amplitude of I_{st} in a concentration-dependent manner (EC_{50} of 2.26 nM) but also shifts V_{peak} to a negative direction by $\sim$15 mV (Figure 2). It was demonstrated in rabbit SA node cells that I_f and $I_{Ca,L}$ are potentiated by ISO in a concentration-dependent manner with an EC_{50} of 13.6 and 7 nM, respectively (Zaza *et al*., 1996). The sensitivity of I_{st} to the β-adrenergic agonist ISO thus appears to be similar or even higher, compared with that of I_f and $I_{Ca,L}$ in SA node cells. Moreover, ISO significantly shifts V_{peak} to a negative direction, producing a pronounced stimulation at potentials within a 20 mV range centered on $\sim$−60 mV (Figure 2d). An increase in SA node automaticity during β-adrenergic stimulation is associated with the acceleration of the slow diastolic depolarization, which drives the membrane potential from the maximal diastolic potential at $\sim$−60 mV towards the threshold for the rapid upstroke of the following action potentials at $\sim$−40 mV (for a review, see DiFrancesco, 1993; Irisawa *et al*., 1993). The β-adrenergic stimulation of I_{st} accompanied by a negative shift of V_{peak} thus appears to be favorable for the contribution of I_{st} to the facilitation of the slow diastolic potential leading to the increase in pace-making activity in SA node cells during elevated sympathetic tone.

It has been demonstrated in mammalian cardiac myocytes that the muscarinic agonist ACh evokes an inhibitory effect on I_f, $I_{Ca,L}$ and I_{Ks} prestimulated by the β-adrenergic agonist ISO (Hescheler *et al*., 1986; DiFrancesco & Tromba, 1988; Harvey & Hume, 1989; Yazawa & Kameyama, 1990; Petit-Jacques *et al*., 1993). Such an accentuated antagonism of ISO stimulation of ion channel activities by ACh is assumed to be mediated through the inhibition of adenylyl cyclase *via* stimulation of pertussis toxin-sensitive G protein G_i and a resultant decrease in intracellular cyclic AMP. The present study confirms that bath application of ACh concentration-dependently ($IC_{50}=133.9$ nM) inhibits I_{st} prestimulated by ISO (Figure 3), which is consistent with the view that I_{st} is regulated through the classical adenylyl cyclase-cyclic AMP cascade (Guo *et al*., 1997). In addition, ACh at a higher concentration (1 μM) evokes a small but significant inhibition of basal I_{st} (10.5±2.0% inhibition, $n=3$). It has been demonstrated in rabbit SA node cells that nanomolar levels of ACh ($IC_{50}=19$ nM) significantly decreases basal I_f by shifting its activation curve in a negative direction, while higher concentrations ($\geqslant$50 nM) of ACh are required to produce a substantial inhibition of basal $I_{Ca,L}$ (DiFrancesco & Tromba, 1988; DiFrancesco *et al*., 1989; Petit-Jacques *et al*., 1993; Zaza *et al*., 1996). Thus, basal I_{st} in guinea-pig SA node cells appears to exhibit less sensitivity to inhibition by ACh than basal I_f and $I_{Ca,L}$ in rabbit SA node cells. Previous workers have provided evidence indicating that the inhibitory effect of ACh on basal I_f and $I_{Ca,L}$ is mediated through inhibition of a high basal adenylyl cyclase activity, leading to a reduction of the

intracellular cyclic AMP level in rabbit SA node cells (DiFrancesco & Tromba, 1988; Petit-Jacques *et al*., 1993). The present investigation thus provides quantitative data for the responses of I_{st} to β-adrenergic and muscarinic agonists and supports the view that I_{st} is autonomically regulated. Further studies are thus required to elucidate fully the intracellular regulatory mechanisms mediating the action of β-adrenergic and muscarinic agonists on I_{st} in SA node cells.

This study was supported by Grant-in-Aid for Scientific Research (Nos. 13670042 and 15590184) from the Japan Society for the Promotion of Science.

References

ANUMONWO, J.M.B., FREEMAN, L.C., KWOK, W.M. & KASS, R.S. (1992). Delayed rectification in single cells isolated from guinea pig sinoatrial node. *Am. J. Physiol.,* **262,** H921–H925.

BÉNITAH, J.-P., GOMEZ, A.M., BAILLY, P., DA PONTE, J.-P., BERSON, G., DELGADO, C. & LORENTE, P. (1993). Heterogeneity of the early outward current in ventricular cells isolated from normal and hypertrophied rat hearts. *J. Physiol. (London),* **469,** 111–138.

DIFRANCESCO, D. (1993). Pacemaker mechanisms in cardiac tissue. *Annu. Rev. Physiol.,* **55,** 455–472.

DIFRANCESCO, D., DUCOURET, P. & ROBINSON, R.B. (1989). Muscarinic modulation of cardiac rate at low acetylcholine concentrations. *Science,* **243,** 669–671.

DIFRANCESCO, D., FERRONI, A., MAZZANTI, M. & TROMBA, C. (1986). Properties of the hyperpolarizing-activated current (i_f) in cells isolated from the rabbit sino-atrial node. *J. Physiol. (London),* **377,** 61–88.

DIFRANCESCO, D. & TROMBA, C. (1988). Inhibition of the hyperpolarization-activated current (i_f) induced by acetylcholine in rabbit sino-atrial node myocytes. *J. Physiol. (London),* **405,** 477–491.

DOERR, T., DENGER, R. & TRAUTWEIN, W. (1989). Calcium currents in single SA nodal cells of the rabbit heart studied with action potential clamp. *Pflügers Arch.,* **413,** 599–603.

FABIATO, A. & FABIATO, F. (1979). Calculator programs for computing the composition of the solutions containing multiple metals and ligands used for experiments in skinned muscle cells. *J. Physiol. (Paris),* **75,** 463–505.

GUO, J. & NOMA, A. (1997). Existence of a low-threshold and sustained inward current in rabbit atrio-ventricular node cells. *Jpn. J. Physiol.,* **47,** 355–359.

GUO, J., MITSUIYE, T. & NOMA, A. (1997). The sustained inward current in sino-atrial node cells of guinea-pig heart. *Pflügers Arch.,* **433,** 390–396.

GUO, J., ONO, K. & NOMA, A. (1995). A sustained inward current activated at the diastolic potential range in rabbit sino-atrial node cells. *J. Physiol. (London),* **483,** 1–13.

GUO, J., ONO, K. & NOMA, A. (1996). Monovalent cation conductance of the sustained inward current in rabbit sinoatrial node cells. *Pflügers Arch.,* **433,** 209–211.

HAGIWARA, N., IRISAWA, H. & KAMEYAMA, M. (1988). Contribution of two types of calcium currents to the pacemaker potentials of rabbit sino-atrial node cells. *J. Physiol. (London),* **395,** 233–253.

HAGIWARA, N., IRISAWA, H., KASANUKI, H. & HOSODA, S. (1992). Background current in sino-atrial node cells of the rabbit heart. *J. Physiol. (London),* **448,** 53–72.

HAMILL, O.P., MARTY, A., NEHER, E., SAKMANN, B. & SIGWORTH, F.J. (1981). Improved patch-clamp techniques for high-resolution current recording from cells and cell-free membrane patches. *Pflügers Arch.,* **391,** 85–100.

HARVEY, R.D. & HUME, J.R. (1989). Autonomic regulation of delayed rectifier K^+ current in mammalian heart involves G proteins. *Am. J. Physiol.,* **257,** H818–H823.

HESCHELER, J., KAMEYAMA, M. & TRAUTWEIN, W. (1986). On the mechanism of muscarinic inhibition of the cardiac Ca current. *Pflügers Arch.,* **407,** 182–189.

IRISAWA, H., BROWN, H.F. & GILES, W. (1993). Cardiac pacemaking in the sinoatrial node. *Physiol. Rev.,* **73,** 197–227.

ISENBERG, G. & KLÖCKNER, U. (1982). Calcium tolerant ventricular myocytes prepared by preincubation in a ''KB medium''. *Pflügers Arch.,* **395,** 6–18.

LEI, M. & BROWN, H.F. (1996). Two components of the delayed rectifier potassium current, I_K, in rabbit sino-atrial node cells. *Exp. Physiol.,* **81,** 725–741.

MANGONI, M.E., COUETTE, B., BOURINET, E., PLATZER, J., REIMER, D., STRIESSNIG, J. & NARGEOT, J. (2003). Functional role of L-type Ca_V 1.3 Ca^{2+} channels in cardiac pacemaker activity. *Proc. Natl. Acad. Sci. U.S.A.,* **100,** 5543–5548.

MATSUURA, H., EHARA, T., DING, W.G., OMATSU-KANBE, M. & ISONO, T. (2002). Rapidly and slowly activating components of delayed rectifier K^+ current in guinea-pig sino-atrial node pacemaker cells. *J. Physiol. (London),* **540,** 815–830.

MITSUIYE, T., SHINAGAWA, Y. & NOMA, A. (2000). Sustained inward current during pacemaker depolarization in mammalian sinoatrial node cells. *Circ. Res.,* **87,** 88–91.

ONO, K. & ITO, H. (1995). Role of rapidly activating delayed rectifier K^+ current in sinoatrial node pacemaker activity. *Am. J. Physiol.,* **269,** H453–H462.

ONO, K., SHIBATA, S. & IIJIMA, T. (2000). Properties of the delayed rectifier potassium current in porcine sino-atrial node cells. *J. Physiol. (London),* **524,** 51–62.

PETIT-JACQUES, J., BOIS, P., BESCOND, J. & LENFANT, J. (1993). Mechanism of muscarinic control of high-threshold calcium current in rabbit sino-atrial node myocytes. *Pflügers Arch.,* **423,** 21–27.

SHINAGAWA, Y., SATOH, H. & NOMA, A. (2000). The sustained inward current and inward rectifier K^+ current in pacemaker cells dissociated from rat sinoatrial node. *J. Physiol. (London),* **523,** 593–605.

TSIEN, R.Y. & RINK, T.J. (1980). Neutral carrier ion-selective microelectrodes for measurement of intracellular free calcium. *Biochim. Biophys. Acta,* **599,** 623–638.

VAN GINNEKEN, A.C.G. & GILES, W. (1991). Voltage clamp measurements of the hyperpolarization-activated inward current I_f in single cells from rabbit sinoatrial node. *J. Physiol. (London),* **434,** 57–83.

VERHEIJCK, E.E., VAN GINNEKEN, A.C.G., BOURIER, J. & BOUMAN, L.N. (1995). Effects of delayed rectifier current blockade by E-4031 on impulse generation in single sinoatrial nodal myocytes of the rabbit. *Circ. Res.,* **76,** 607–615.

VERHEIJCK, E.E., VAN GINNEKEN, A.C.G., WILDERS, R. & BOUMAN, L.N. (1999). Contribution of L-type Ca^{2+} current to electrical activity in sinoatrial nodal myocytes of rabbits. *Am. J. Physiol.,* **276,** H1064–H1077.

YAZAWA, K. & KAMEYAMA, M. (1990). Mechanism of receptor-mediated modulation of the delayed outward potassium current in guinea-pig ventricular myocytes. *J. Physiol. (London),* **421,** 135–150.

ZAZA, A., ROBINSON, R.B. & DIFRANCESCO, D. (1996). Basal responses of the L-type Ca^{2+} and hyperpolarization-activated currents to autonomic agonists in the rabbit sino-atrial node. *J. Physiol. (London),* **491,** 347–355.

ZHANG, H., HOLDEN, A.V. & BOYETT, M.R. (2002). Sustained inward current and pacemaker activity of mammalian sinoatrial node. *J. Cardiovasc. Electrophysiol.,* **13,** 809–812.

(Received October 15, 2004
Revised November 17, 2004
Accepted November 18, 2004)